

Intracellular calcium measurements as a method in studies on activity of purinergic P2X receptor channels

Mu-Lan He,* Hana Zemkova,* Taka-aki Koshimizu, Melanija Tomić, and Stanko S. Stojilkovic

Endocrinology and Reproduction Research Branch, National Institute of Child Health and Human Development, National Institutes of Health, Bethesda, Maryland 20892-4510

Submitted 29 January 2003; accepted in final form 22 April 2003

He, Mu-Lan, Hana Zemkova, Taka-aki Koshimizu, Melanija Tomić, and Stanko S. Stojilkovic. Intracellular Ca^{2+} measurements as a method in studies on activity of purinergic P2X receptor channels. *Am J Physiol Cell Physiol* 285: C467–C479, 2003. First published April 23, 2003; 10.1152/ajpcell.00042.2003.—Extracellular nucleotide-activated purinergic receptors (P2XRs) are a family of cation-permeable channels that conduct small cations, including Ca^{2+} , leading to the depolarization of cells and subsequent stimulation of voltage-gated Ca^{2+} influx in excitable cells. Here, we studied the spatiotemporal characteristics of intracellular Ca^{2+} signaling and its dependence on current signaling in excitable mouse immortalized gonadotropin-releasing hormone-secreting cells (GT1) and nonexcitable human embryonic kidney cells (HEK-293) cells expressing wild-type and chimeric P2XRs. In both cell types, P2XR generated depolarizing currents during the sustained ATP stimulation, which desensitized in order (from rapidly desensitizing to nondesensitizing): $\text{P2X}_3\text{R} > \text{P2X}_{2b} + \text{X}_4\text{R} > \text{P2X}_{2b}\text{R} > \text{P2X}_{2a} + \text{X}_4\text{R} > \text{P2X}_4\text{R} > \text{P2X}_{2a}\text{R} > \text{P2X}_7\text{R}$. HEK-293 cells were not suitable for studies on P2XR-mediated Ca^{2+} influx because of the coactivation of endogenously expressed Ca^{2+} -mobilizing purinergic P2Y receptors. However, when expressed in GT1 cells, all wild-type and chimeric P2XRs responded to agonist binding with global Ca^{2+} signals, which desensitized in the same order as current signals but in a significantly slower manner. The global distribution of Ca^{2+} signals was present independently of the rate of current desensitization. The temporal characteristics of Ca^{2+} signals were not affected by voltage-gated Ca^{2+} influx and removal of extracellular sodium. Ca^{2+} signals reflected well the receptor-specific EC_{50} values for ATP and the extracellular Zn^{2+} and pH sensitivities of P2XRs. These results indicate that intracellular Ca^{2+} measurements are useful for characterizing the pharmacological properties and messenger functions of P2XRs, as well as the kinetics of channel activity, when the host cells do not express other members of purinergic receptors.

ATP-gated receptor channels; inward currents; intracellular calcium signals; desensitization-inactivation; voltage-gated calcium influx; localized and global calcium signals

ATP-GATED PURINERGIC RECEPTOR CHANNELS (P2XRs) are expressed in many nonexcitable and excitable cells,

*M.-L. He and H. Zemkova contributed equally to this work.

Address for reprint requests and other correspondence: S. Stojilkovic, Section on Cellular Signaling, ERRL/NICHD/NIH, Bldg. 49, Rm. 6A-36, 49 Convent Drive, Bethesda, MD 20892-4510 (E-mail: stankos@helix.nih.gov).

including neurons, neuroendocrine and endocrine cells, epithelia, endothelia, bone, muscle, and hemopoietic tissues (28). These receptor channels participate in the control of numerous cellular functions, such as neurotransmission, hormone secretion, transcriptional regulation, and protein synthesis (30). The major physiological mechanism by which activated P2XRs control cellular functions is elevation in intracellular Ca^{2+} concentration ($[\text{Ca}^{2+}]_i$). The pores of all P2XRs are permeable to small monovalent and divalent cations, including significant permeability to Ca^{2+} (12, 13, 35, 39, 42). In nonexcitable cells, Ca^{2+} influx through the pores of channels is the most important, if not exclusive, pathway for Ca^{2+} signaling. In excitable cells, activated receptors also promote voltage-gated Ca^{2+} influx due to ion influx-induced depolarization of cell membrane (24).

Although $[\text{Ca}^{2+}]_i$ measurements are sensitive enough to record the activity of native and recombinant P2XR in single nonexcitable and excitable cells (22, 32, 38, 43, 47), the majority of studies with P2XRs are done using current measurements (28, 30). Patch-clamp techniques provide powerful tools in evaluating the status of P2XR pores and thus are extremely useful in biophysical characterization of these receptors. With respect to physiology and pharmacology of P2XR, Ca^{2+} rather than current measurements have potential to provide valuable information. $[\text{Ca}^{2+}]_i$ measurements were also occasionally used in evaluating the kinetics of receptor activity (2, 16, 20, 22, 24). The main advantage in using single-cell $[\text{Ca}^{2+}]_i$ imaging in such studies is that measurements can be done simultaneously in tens of cells, enabling reliable statistical analysis, whereas current measurements are done in one cell per experiment, and slow recovery of receptors from desensitization makes repeated measurements in the same cell difficult. Single-cell $[\text{Ca}^{2+}]_i$ imaging provides the same advantages in studies on pharmacological profiles of P2XRs and testing new compounds. Because Ca^{2+} signaling by P2XRs is incompletely characterized, however, $[\text{Ca}^{2+}]_i$ measurements could be viewed as an inadequate method for studies on physiology, pharmacology, and kinetics of P2XR activity.

The costs of publication of this article were defrayed in part by the payment of page charges. The article must therefore be hereby marked "advertisement" in accordance with 18 U.S.C. Section 1734 solely to indicate this fact.

Here, we studied the spatiotemporal aspects of ATP-induced Ca^{2+} signals in P2XR-expressing cells and the dependence of the pattern of Ca^{2+} signaling on the kinetics of channel activity. Experiments were done with several wild-type and chimeric P2XRs in homomeric configuration. The selection of P2XRs was based on the kinetics of their desensitization during the sustained ATP stimulation, from rapidly desensitizing P2X₃R to nondesensitizing P2X₇R. These include the recently constructed P2X_{2a}R + X₄R and P2X_{2b} + X₄R chimeras, having the Val⁶⁶-Tyr³¹⁵ ectodomain sequence of P2X₄R in the backbones of P2X_{2a}R and P2X_{2b}R and differing from parental receptors with respect to rates of signal desensitization (17). To express P2XRs, we selected two cell types: nonexcitable human embryonic kidney cells (hereafter HEK-293 cells) and excitable mouse immortalized gonadotropin-releasing hormone-secreting cells (hereafter GT1 cells). Because the majority of previous studies with recombinant P2XR currents were done in HEK-293 cells (4, 14, 26, 27, 36, 46), we used these cells for current measurements to provide a valid comparison with the literature.

Initially, we characterized the extent to which the P2XR current properties differ in the two selected cell types. In further studies, we focused on the spatiotemporal characteristics of Ca^{2+} signaling by P2XRs expressed in GT1 cells, because the coactivation of endogenously expressed G protein-coupled P2YRs in HEK-293 cells (31) interferes with measurements of P2XR-mediated Ca^{2+} influx. We also compared the peak current and $[\text{Ca}^{2+}]_i$ responses (commonly used for calculating the EC₅₀ and IC₅₀ values) and the rates of signal desensitization during prolonged ATP stimulation. In the final stage, we analyzed the usefulness of Ca^{2+} measurements as a method in studies on pharmacological properties of P2XRs. The results indicate that single-cell Ca^{2+} measurements not only provide a valuable method for characterizing the spatiotemporal aspects of Ca^{2+} signaling by P2XRs, but the relationship between current and Ca^{2+} and the sensitivity of Ca^{2+} signals to changes in extracellular pH and Zn^{2+} concentrations proves them to be useful in studies on channel activity.

MATERIALS AND METHODS

DNA constructs, cell culture, and transfection. The coding sequences of the rat P2X_{2a}, P2X_{2b}, P2X₃, P2X₄, and P2X₇ subunits, isolated by RT-PCR from pituitary, were subcloned into the bicistronic enhanced fluorescent protein expression vector, pIRES2-EGFP (Clontech, Palo Alto, CA), as described previously (19). P2X_{2a} + X₄R and P2X_{2b} + X₄R chimeras were directly constructed by overlap extension PCR by using the corresponding wild-type P2XR cDNA as templates. Mutagenesis primers were pairs of chimeric sense and antisense that were 36-mer long, with the joint sites positioned in the center, i.e., 18 nucleotides of P2X₂ or P2X₄ to each side, as described in He et al. (17). The constructed chimeric subunits contain the Val⁶⁶-Tyr³¹⁵ extracellular domain of P2X₄R instead of the native sequence Ile⁶⁶-Tyr³¹⁰ of P2X₂R. These

chimeric P2XRs were also subcloned into GFP-expression vector pIRES2-EGFP. The identity of all constructs was verified by dye terminator cycle sequencing (Perkin Elmer, Foster City, CA), performed by the Laboratory of Molecular Technology (NCI, Frederick, MD). The large-scale plasmid DNAs for transfection were prepared using a QIAGEN Plasmid Maxi kit (Qiagen, Germany).

GT1 cells and HEK-293 cells were used to examine the patterns of desensitization in P2XRs as previously described (19). GT1 cells were routinely maintained in Dulbecco's modified Eagle's medium/Ham's F-12 medium (1:1), containing 10% (vol/vol) fetal bovine serum and 100 $\mu\text{g}/\text{ml}$ gentamicin (Invitrogen, Carlsbad, CA) in a water-saturated atmosphere of 5% CO_2 -95% air at 37°C. HEK-293 cells were cultured in MEM supplemented with 10% horse serum and 100 $\mu\text{g}/\text{ml}$ gentamicin. Before the day of transfection, cells were plated on 25-mm poly-L-lysine (0.01% wt/vol; Sigma, St. Louis, MO)-coated coverslips at a density of $0.75\text{--}1 \times 10^5$ cells per 35-mm dish. For each dish of cells, transient transfection of expression constructs was conducted using 1 μg of DNA and 7 μl of Lipofectamine 2000 Reagent (Invitrogen) in 3 ml of serum-free Opti-MEM. After 6 h of incubation, transfection mixture was replaced with normal culture medium. Cells were subjected to experiments 24–48 h after transfection.

Ca^{2+} measurements. Transfected GT1 cells were preloaded with 1 μM fura 2 acetoxyethyl ester (fura 2-AM; Molecular Probe, Eugene, OR) for 60 min at room temperature in modified Krebs Ringer buffer [(in mM) 120 NaCl, 5 KCl, 1.2 CaCl_2 , 0.7 MgSO_4 , 15 *N*-2-hydroxyethylpiperazine-*N'*-2-ethanesulfonic acid (HEPES), and 1.8 g/l glucose (pH 7.4)]. After dye loading, cells were washed in the same medium and kept in the dark for at least 30 min before single-cell $[\text{Ca}^{2+}]_i$ measurements. Coverslips with cells were mounted on the stage of an Axiovert 135 microscope (Carl Zeiss, Oberkochen, Germany) attached to the Attofluor digital fluorescence microscopy system (Atto Instruments, Rockville, MD). All cells were stimulated with 100 μM ATP, and the dynamic changes of $[\text{Ca}^{2+}]_i$ were examined under a $\times 40$ oil immersion objective during exposure to alternating 340- and 380-nm light beams, and the intensity of light emission at 520 nm was measured. The ratio of light intensities, F_{340}/F_{380} , which reflects changes in $[\text{Ca}^{2+}]_i$, was simultaneously followed in 15–50 single cells at a rate of ~ 1 point/s. Spatial resolution was estimated to be ~ 1 μm . All experiments were done at room temperature.

Current measurements. Electrophysiological experiments were performed on GT1 and HEK-293 cells at room temperature using whole cell patch-clamp recording techniques (15). ATP-induced currents were recorded using an Axopatch 200B patch-clamp amplifier (Axon Instruments, Union City, CA) and filtered at 2 kHz using a low-pass Bessel filter. Forty to seventy percent series resistance compensation was used. Patch electrodes, fabricated from borosilicate glass (type 1B150F-3; World Precision Instruments, Sarasota, FL) using a Flaming Brown horizontal puller (P-87; Sutter Instruments, Novato, CA), were heat polished to a final tip resistance of 3–5 $\text{M}\Omega$. All current records were captured and stored using the pCLAMP 8 software packages in conjunction with the Digidata 1322A analog-to-digital converter (Axon Instruments). Patch electrodes were filled with a solution containing (in mM) 140 KCl, 0.5 CaCl_2 , 1 MgCl_2 , 5 EGTA, and 10 HEPES, pH adjusted with 1 M KOH to 7.2. The osmolarity of the internal solutions was 282–287 mosM. The bath solution contained (in mM) 142 NaCl, 3 KCl, 1 MgCl_2 , 2 CaCl_2 , 10 glucose, and 10 HEPES, pH adjusted to 7.4 with 1

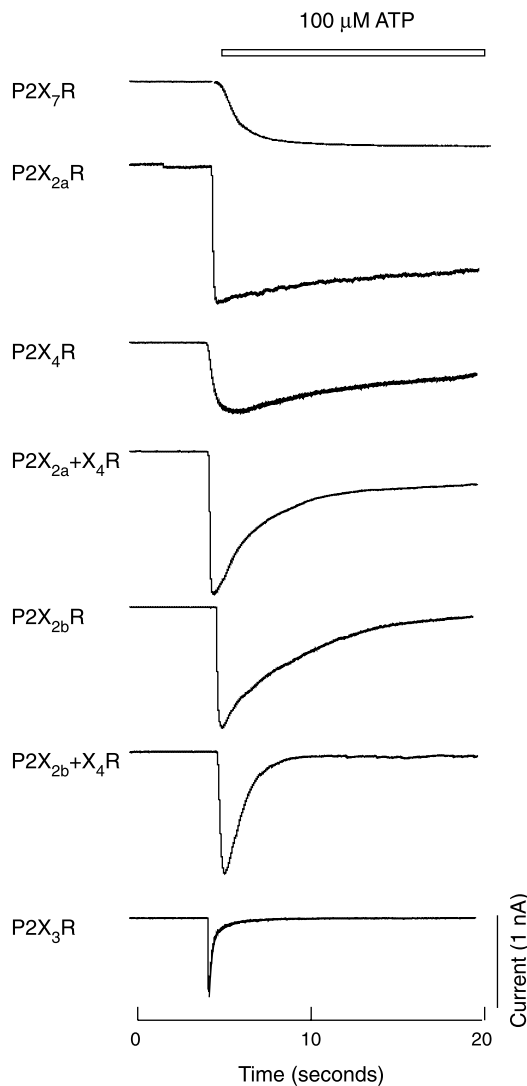


Fig. 1. The receptor-specific pattern of ATP-induced current signals in HEK-293 cells expressing extracellular nucleotide-activated purinergic receptors (P2XRs). Experimental records are representative of at least 5 traces per receptor type. Means \pm SE for peak current responses are shown in Table 1. In this and following figures, horizontal bars indicate the exposure time to 100 μ M ATP and the current traces shown are from cells clamped at -60 mV.

M NaOH. The osmolarity of this solution was 285–295 mosM. A 3 M KCl-agar bridge was placed between the bathing solution and the reference electrode. ATP was applied for 60 s using a fast gravity-driven microperfusion system

(BPS-8; ALA Scientific Instruments). The application tip was routinely positioned ~ 500 μ m above the recorded cell. Less than 600 ms was required for complete exchange of solutions around the patched cells, as estimated from altered potassium current (10–90% rise time). All experiments were done at room temperature.

Calculations. The time course of the $[Ca^{2+}]_i$ and current evoked by sustained ATP stimulation were fitted to a single exponential function ($ae^{-kt} + b$) using GraphPad Prism (GraphPad Software, San Diego, CA) and pCLAMP 8, respectively, to generate the half-time for signal desensitization ($\tau = \ln 2/k$). Linear and log-linear regression analyses were used to correlate variables, and the strength of correlation was expressed as Pearson's R coefficient (KaleidaGraph, Reading, PA). Significant differences, with $P < 0.05$, were determined by one-way ANOVA with Newman-Keuls multiple-comparison test. Each experiment was repeated five or more times to ensure the reproducibility of the findings.

RESULTS

Receptor- and cell type-specific responses. ATP-induced currents were measured using whole cell patch-recording mode in HEK-293 and GT1 cells expressing homomeric P2XRs. In both cell types, activation of all channel subtypes by ATP evoked depolarizing inward currents. The pattern of current response during the sustained ATP stimulation was specific for the expressed receptor subtype and was not affected by changing the host cells. Figure 1 illustrates typical patterns of current responses by seven receptors expressed in HEK-293 cells. Current desensitized rapidly in P2X₃R- and P2X_{2b} + X₄R-expressing cells, with moderate rates in P2X_{2b}R-, P2X_{2a}+X₄R-, and P2X₄R-expressing cells, slowly in P2X_{2a}R-expressing cells, and did not desensitize in P2X₇R-expressing cells. ATP-induced currents by P2XR expressed in GT1 cells desensitized in the same order as in HEK-293 cells. The rates of their desensitization were also comparable in two cell types. Figure 2 shows the pattern of current responses in HEK-293 (B) and GT1 (A) cells expressing P2X_{2a}R and P2X_{2b}R, and mean values for half times of current desensitization are shown.

In further studies, we compared the potential usefulness of two cell types for analyzing the P2XR activity by single-cell Ca^{2+} measurements. Native HEK-293 cells do not express voltage-gated Ca^{2+} channels, as indicated by inability of high-potassium-induced depolarization of cells to elevate $[Ca^{2+}]_i$ (Fig. 3A, left upper trace), whereas depolarization of GT1 cells increased

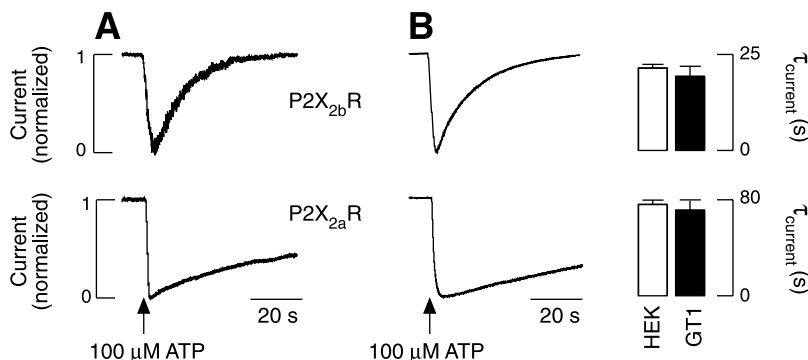


Fig. 2. Comparison of the pattern of current signals in HEK-293 (B) and GT1 (A) cells expressing P2X_{2a}R (lower traces) and P2X_{2b}R (upper traces) in response to 100 μ M ATP. Peak amplitudes of current responses were normalized. Bars indicate means \pm SE for half-time (τ) values, which were calculated as stated in MATERIALS AND METHODS.

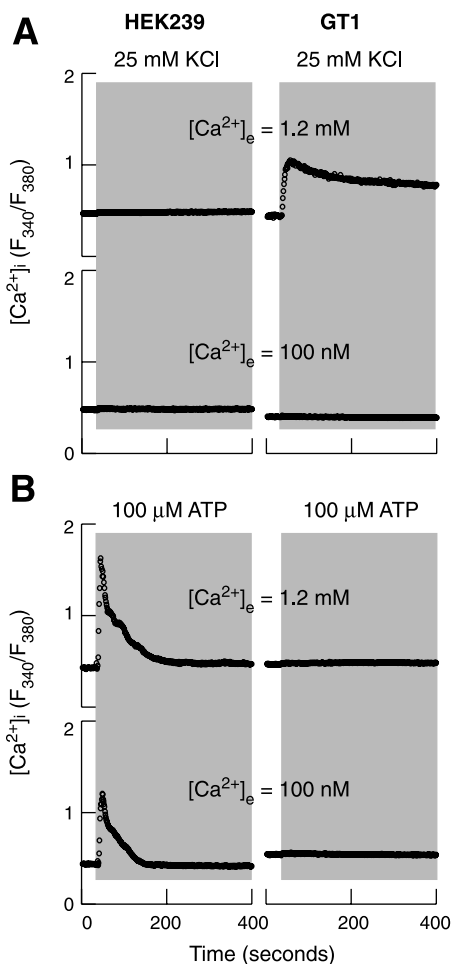


Fig. 3. Characterization of native HEK-293 and GT1 cells for Ca^{2+} measurements. **A:** the lack of effects of high-potassium-induced depolarization of HEK-293 cells on intracellular calcium concentration ($[\text{Ca}^{2+}]_i$) (left), and extracellular Ca^{2+} -dependence of high-potassium-induced rise in $[\text{Ca}^{2+}]_i$ in GT1 cells (right). **B:** 100 μM ATP-induced rise in $[\text{Ca}^{2+}]_i$ in native HEK-293 cells in Ca^{2+} -containing (upper trace) and Ca^{2+} -deficient medium (bottom trace) (left), and the lack of effects of 100 μM ATP on $[\text{Ca}^{2+}]_i$ in GT1 cells (right). In this and the following experiments, cells were loaded with fura 2, and recordings were done in Krebs-Ringer buffer with 1.2 mM Ca^{2+} . Experimental data are shown by circles and are mean values from at least 15 records in representative experiments.

the $[\text{Ca}^{2+}]_i$ (Fig. 3A, right upper trace). The response was abolished by removal of extracellular Ca^{2+} (Fig. 3A, right bottom trace). On the other hand, ATP induced a rapid and transient increase in $[\text{Ca}^{2+}]_i$ in HEK-293 cells, but not in GT1 cells, bathed in Ca^{2+} -containing (Fig. 3B, left upper trace) and Ca^{2+} -deficient (left bottom trace) medium. These results confirm that native HEK-293 cells express Ca^{2+} -mobilizing P2Y purinergic receptors (31) and, thus, are not a good cell model for measurements of P2XR-mediated Ca^{2+} influx.

In additional experiments, we further characterized GT1 cells as a potential cell model for studies on activity of P2XRs. ATP-induced elevation in the $[\text{Ca}^{2+}]_i$ in GT1 cells expressing P2X_{2a}R was abolished by removal of extracellular Ca^{2+} , indicating that Ca^{2+} in-

flux exclusively accounts for the rise in $[\text{Ca}^{2+}]_i$ (Fig. 4A). The substitution of extracellular Na^+ with *N*-methyl-D-glucamine reduced the amplitude of Ca^{2+} signals but did not affect the rates of Ca^{2+} signal desensitization (Fig. 4B). This is probably the receptor-specific feature, because an increase in peak amplitude of Ca^{2+} signals was observed in P2X₄R-expressing cells bathed in sodium-deficient medium (47).

We also tested the impact of expression of voltage-gated Ca^{2+} channels on the pattern of ATP-induced Ca^{2+} signaling. These experiments were done in P2X_{2a}R-expressing cells. The addition of nifedipine, a blocker of L-type Ca^{2+} channels, also reduced the amplitude of Ca^{2+} responses without affecting the rates of signal desensitization (Fig. 4C, middle trace). Activation of voltage-gated Ca^{2+} influx by high-potassium-induced depolarization of cells before ATP stimulation was also ineffective in changing the rates of Ca^{2+} signal desensitization (Fig. 4C, bottom trace). To test the potential coupling of Ca^{2+} influx with Ca^{2+} -induced Ca^{2+} release from intracellular pools, cells were treated with 100 μM ryanodine. The pattern of ATP-induced Ca^{2+} signals in ryanodine-treated cells was indistinguishable from that observed in control cells (not shown), confirming a previously published finding that these cells do not express operative ryanodine receptor channels (5).

Spatiotemporal characteristics of P2XR-generated Ca^{2+} signals in GT1 cells. As in current responses by recombinant P2XRs, ATP-induced Ca^{2+} response was composed of two phases: a relatively rapid rise in $[\text{Ca}^{2+}]_i$ from basal levels to peak response (activation phase), followed by a gradual decline toward the plateau response (desensitization phase) (Fig. 4A). In further studies, we examined whether the temporal patterns of Ca^{2+} signaling by recombinant P2XRs reflect the receptor specificity of current signaling. We also examined the spatial characteristics of P2XR-generated Ca^{2+} signals during activation and desensitization phases. In these and following experiments, voltage-gated Ca^{2+} influx was not blocked and all receptors were stimulated with 100 μM ATP unless otherwise indicated.

Figure 5A shows that P2XR-generated Ca^{2+} signals were receptor specific with respect to the peak Ca^{2+} responses and signal desensitization rates. The peak amplitudes were in the following order: P2X₃R < P2X₇R < P2X₄R = P2X_{2b} + X₄R < P2X_{2a} + X₄R < P2X_{2b}R < P2X_{2a}R (Table 1). In parallel to current responses to 100 μM ATP (Fig. 1), Ca^{2+} signals desensitized very rapidly in P2X₃R- and P2X_{2b} + X₄R-expressing cells and with moderate rates in P2X_{2b}R-, P2X_{2a} + X₄R-, and P2X₄R-expressing cells, whereas Ca^{2+} signals showed little or no desensitization in P2X_{2a}R and P2X₇R-expressing cells. Figure 5B shows ratio images of cells before addition of agonist (left) and at the peak $[\text{Ca}^{2+}]_i$ response (right). There was an increase in F₃₄₀/F₃₈₀ ratio in all regions of the central section of cells expressing all of the examined channels, indicating that generation of global Ca^{2+} signals is a common feature of these receptors.

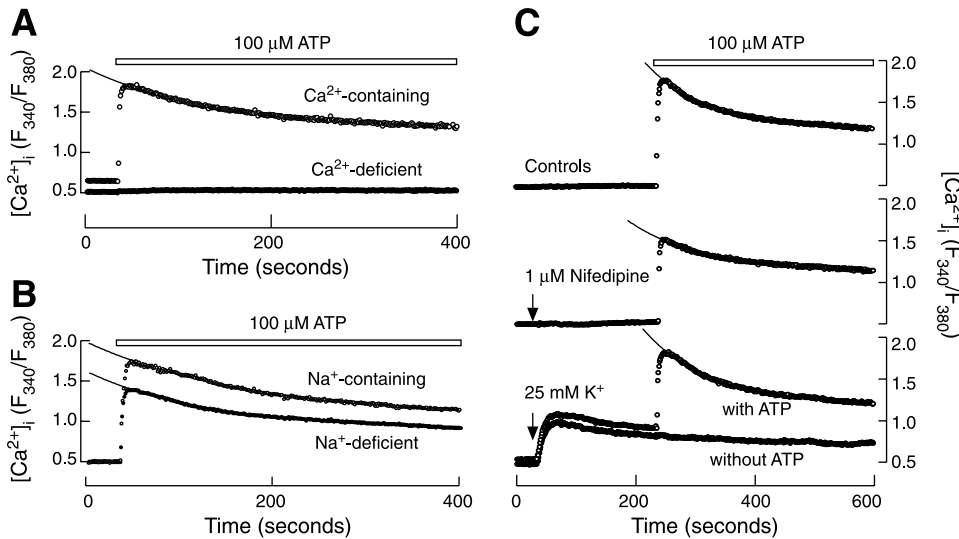


Fig. 4. Characterization of Ca^{2+} signaling in GT1 cells expressing P2X_{2a}R. A: extracellular Ca^{2+} dependence of 100 μM ATP-induced Ca^{2+} signals. B: extracellular sodium independence of ATP-induced Ca^{2+} signals. In this experiment, sodium was substituted with equimolar *N*-methyl-D-glucamine. C: typical profiles of ATP-induced Ca^{2+} signals in controls (upper trace), in cells with blocked L-type Ca^{2+} channels by nifedipine (middle trace), and in high-potassium-depolarized cells (bottom trace, open circles). In this and following experiments, fitted curves are shown by full lines and are extrapolated for clarity.

Except for P2X₇R, activation phase was too rapid to be analyzed by the imaging system with the resolution time of about one image per second. Figure 6 illustrates the spatiotemporal aspects of Ca^{2+} signals in P2X₇R-expressing cells before and during activation of receptors with 1 mM ATP. The temporal changes of Ca^{2+} signal (Fig. 6, bottom right) are shown as F_{340}/F_{380} ratio of averaged intensities in the whole cell area. The $[Ca^{2+}]_i$ rose during continuous ATP stimulation, reaching the plateau 25 s after the addition of ATP. Fig. 6, top, shows several ratio images taken at different time points (denoted by red circles at lower right). Consistent with the generation of global Ca^{2+} signals during activation phase, there was an increase in the ratio in all regions of the central section of the cell.

The receptor-specific rates of desensitization did not affect the global nature of Ca^{2+} signaling. Figure 7 illustrates spatial characteristics of Ca^{2+} signaling in P2X_{2a}R (Fig. 7A), P2X_{2b}R (Fig. 7B), and P2X₃R (Fig. 7C). After reaching the peak value, the $[Ca^{2+}]_i$ declined slowly to the steady level in P2X_{2a}R-expressing cells, at moderate rates in P2X_{2b}R-expressing cells, and rapidly in P2X₃R-expressing cells. In all three cases, the ratio values in all areas in the central section of the cells decreased but remained above the basal level, suggesting that the global nature of Ca^{2+} signals was preserved during receptor desensitization.

Comparison of Ca^{2+} and current signaling in P2XR-expressing cells. To study the concentration-dependent effects of ATP on peak amplitude of current and Ca^{2+} responses, we selected P2X_{2a}R-expressing cells. In both measurements, ATP was effective in the 0.5–100 μM concentration range (Fig. 8A). The parallelism in the concentration-dependent curves for current and Ca^{2+} responses indicates that the peak amplitude of Ca^{2+} signals reflects well the size of currents.

In cells expressing different P2XRs and stimulated with 100 μM ATP, there were significant variations in the amplitudes of peak current/ Ca^{2+} responses (Table 1). Overall, the peak amplitudes of current and Ca^{2+} responses correlated reasonably well ($R = 0.88$ for

linear relationship; Fig. 8B), further indicating that the amplitude of current response represents the major factor that determines the magnitude of Ca^{2+} signals. We also correlated the receptor-specific half-times of current desensitization (τ) with the normalized amplitude of $[Ca^{2+}]_i$ responses. To do this, the peak amplitudes of $[Ca^{2+}]_i$ response were divided with the peak amplitudes of the corresponding currents and these values were plotted against calculated τ for current desensitization. Results, shown in Fig. 8C, indicate a strong ($R = 0.97$) log-linear relationship between decay in current responses and peak amplitude of normalized $[Ca^{2+}]_i$ responses. These results imply that, in addition to the size of current, the rate of current desensitization influences the peak amplitude of $[Ca^{2+}]_i$ response, especially in rapidly desensitizing channels.

In further studies, we compared the rates in current and Ca^{2+} signal desensitization during the prolonged ATP stimulation. A closer evaluation of the current and Ca^{2+} decays in cells expressing four wild-type and two chimeric P2XRs is shown in Fig. 9A. Both Ca^{2+} and current measurements revealed the receptor-specific desensitization pattern in order (from rapidly desensitizing to nondesensitizing): P2X₃R > P2X_{2b} + X₄R > P2X_{2b}R > P2X_{2a} + X₄R > P2X₄R > P2X_{2a}R > P2X₇R. In chimeric P2X_{2a} + X₄R and P2X_{2b} + X₄R, substitutions of P2X₂R ectodomain to that of P2X₄ apparently accelerated desensitization rates, and these functional differences were detected in both Ca^{2+} and current measurements.

The calculated τ values were consistently smaller in current measurements than in $[Ca^{2+}]_i$ measurements (Fig. 9B and Table 2), indicating that intracellular Ca^{2+} handling mechanisms influence the rates of signal decrease. Correlation analysis of τ values for current and Ca^{2+} decays showed a strong linear relationship, with a fourfold higher τ for $[Ca^{2+}]_i$ signals (Fig. 9B). Two chimeric receptors fit well into the curve (Fig. 9B, filled circles), further indicating that modification of the receptor structure affects the rates of their desensitization but does not change the impact of Ca^{2+} handling on sig-

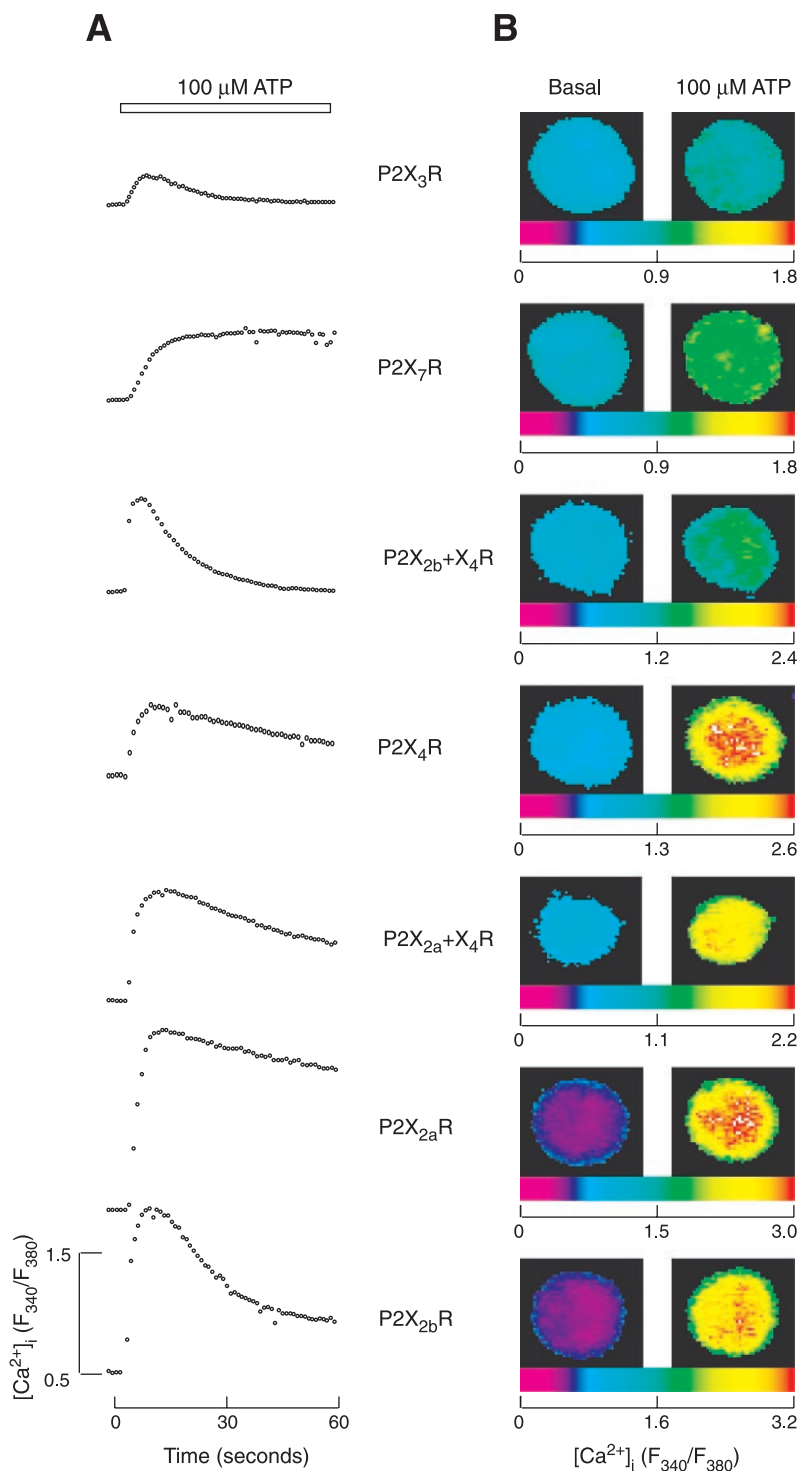


Fig. 5. Common and receptor-specific characteristics of Ca^{2+} signaling by wild-type and chimeric P2XRs expressed in GT1 cells. *A*: the receptor-specific temporal patterns of 100 μM ATP-induced Ca^{2+} signals in cells expressing different P2XRs. The traces shown are mean values from at least 15 records in representative experiments. Means \pm SE for peak Ca^{2+} responses are shown in Table 1. *B*: spatial distribution of Ca^{2+} signals at the peak Ca^{2+} response. For each channel, ratio images of cells were obtained before the addition of 100 μM ATP (*left*) and at the peak of response (*right*). The horizontal bars below images indicate the pseudocolor scale for each experiment.

naling. Thus the slower kinetics of Ca^{2+} elimination from the cytosol is not dependent on the channel type.

Effects of extracellular pH and Zn^{2+} on ATP-induced Ca^{2+} signaling. To test the validity of Ca^{2+} measurements as a method in studies on pharmacological properties of P2XRs, we examined the sensitivity of ATP-induced Ca^{2+} responses in GT1 cells to extracellular pH and Zn^{2+} . In accord with experiments with current measurements (18, 34, 44), acidification and alkalin-

ization had opposite effects on ATP-induced Ca^{2+} responses in P2X_{2a}R- and P2X₄R-expressing cells. As shown in Fig. 10, acidification increased the amplitude of Ca^{2+} responses in P2X_{2a}R-expressing cells stimulated with 1 μM ATP, whereas in alkalinized cells the response was diminished. In P2X₄R-expressing cells, however, acidification attenuated 1 μM ATP-induced Ca^{2+} response and alkalinization facilitated response, compared with physiological pH 7.4.

Table 1. Peak amplitudes of 100 μM ATP-induced calcium and current responses

Receptor	$[\text{Ca}^{2+}]_i$ (F_{340}/F_{380})	Current, nA
P2X ₇ R	0.82 ± 0.07 (8)	0.80 ± 0.10 (5)
P2X _{2a} R	1.78 ± 0.17 (12)	1.89 ± 0.24 (14)
P2X ₄ R	1.05 ± 0.07 (11)	1.11 ± 0.24 (11)
P2X _{2a} R + X ₄ R	1.35 ± 0.15 (7)	2.09 ± 0.45 (19)
P2X _{2b} R	1.41 ± 0.09 (14)	1.99 ± 0.46 (13)
P2X _{2b} R + X ₄ R	1.13 ± 0.23 (5)	2.08 ± 0.67 (12)
P2X ₃ R	0.43 ± 0.06 (7)	0.98 ± 0.16 (19)

Numbers in parenthesis indicate number of single cells for current recordings or number of experiments with simultaneous calcium recordings with at least 15 cells per dish. The basal intracellular calcium concentration ($[\text{Ca}^{2+}]_i$) and leak currents were subtracted.

ATP-induced Ca^{2+} signals also reflected well the extracellular Zn^{2+} sensitivity of P2X_{2a}R (9, 45). When added in 10 μM concentration for 3–5 min before ATP stimulation, Zn^{2+} increased the sensitivity of P2X_{2a}R, which is illustrated in Fig. 11A by change in the threshold concentrations of agonist (*left traces*) and increase in the amplitude of Ca^{2+} response to 1 μM ATP (*right traces*). The full concentration dependence of ATP on peak amplitude of Ca^{2+} signals and the leftward shift in EC_{50} (from 1.81 ± 0.03 μM to 0.35 ± 0.03 μM) is shown in Fig. 11B. Increase in the sensitivity of P2X_{2a}R for ATP was accompanied with increase in the rates of signal desensitization (Fig. 11C), confirming that efficacy of agonist for the ligand binding domain reflects the strength of desensitization (16, 17).

DISCUSSION

Here, we studied the spatiotemporal aspects of Ca^{2+} signaling by P2XRs, the dependence of Ca^{2+} signaling pattern on the kinetics of current activation and desensitization, and the validation of single-cell Ca^{2+} measurements as a method for investigating the P2XR activity. For current measurements, we used HEK-293 and GT1 cells. A majority of previously published electrophysiological recordings with recombinant P2XRs was done in HEK-293 cells (4, 14, 26, 27, 36, 46), and we used these cells in current recordings to provide a valuable control for comparison with previous work. In full accordance with literature data (reviewed in Refs.

28 and 30), we show here that wild-type P2XRs desensitized in a receptor-specific manner. P2X₃R desensitized rapidly, P2X_{2b}R desensitized with moderate rates, P2X_{2a}R desensitized slowly, and P2X₇R did not desensitize. Furthermore, two chimeric channels, P2X_{2a}R + X₄R and P2X_{2b}R + X₄R, desensitized in a manner that differed from that observed in parental receptors. Finally, the patterns of ATP-induced current signaling in mammalian HEK-293 and GT1 cells were highly comparable. The receptor-specific current responses in these two cell types were also comparable with records from receptors expressed in *Xenopus* oocytes (3, 6, 33, 46), further suggesting that the influence of host cells is not critical in evaluating the receptor-specific activity by current measurements.

For Ca^{2+} measurements, we used immortalized gonadotropin-releasing hormone-secreting GT1, but not HEK-293 cells. Consistent with an earlier published study showing the expression of P2YRs in HEK-293 cells (31) and high amplitude but transient nature of Ca^{2+} signaling in other cell types expressing P2YRs (47), we show that ATP-induced peak Ca^{2+} mobilization in these cells exceeds or is comparable in magnitude and/or duration with Ca^{2+} influx by all P2XRs other than P2X_{2a}R and P2X₇R. The sensitivity of these receptors to ATP and several other agonists is in the concentration range typical for P2XRs (30). Thus Ca^{2+} measurements in these cells could not be effectively used to study P2XR-mediated Ca^{2+} influx. In contrast, GT1 cells do not express purinergic P1 and P2 receptors endogenously (21). Together with high expression efficiency for P2XRs (>70%), this provides the major advantage for their selection in this and related (16, 17, 23) studies.

GT1 cells have several other major advantages for studies on P2XR activity. The endogenous ectoATPase activity in GT1 cells is low (Tomić et al., unpublished observations) compared with other neuroendocrine cells (37), a feature important for experiments with sustained ATP stimulation. The secretory pathway in GT1 cells is operative (25) and provides the potential for studies on the coupling of P2XR to exocytosis. GT1 cells (but not HEK-293 cells) express voltage-gated Ca^{2+} channels and spontaneously fire dihydropyridine-sensitive action potentials (40, 41). Because P2XRs are frequently expressed in excitable cells and

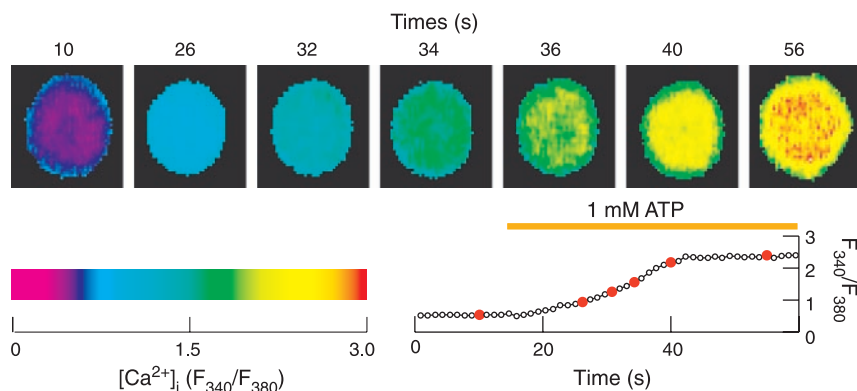


Fig. 6. Spatiotemporal characteristics of Ca^{2+} signaling during the activation phase of P2X₇R. *Top* shows ratio (F_{340}/F_{380}) images of a single cell at 7 different time points from a representative experiment. The pseudocolor scale is shown at *bottom left*. *Bottom right* shows temporal changes of $[\text{Ca}^{2+}]_i$ recorded from the whole cell area. Red circles correspond to images at *top*.

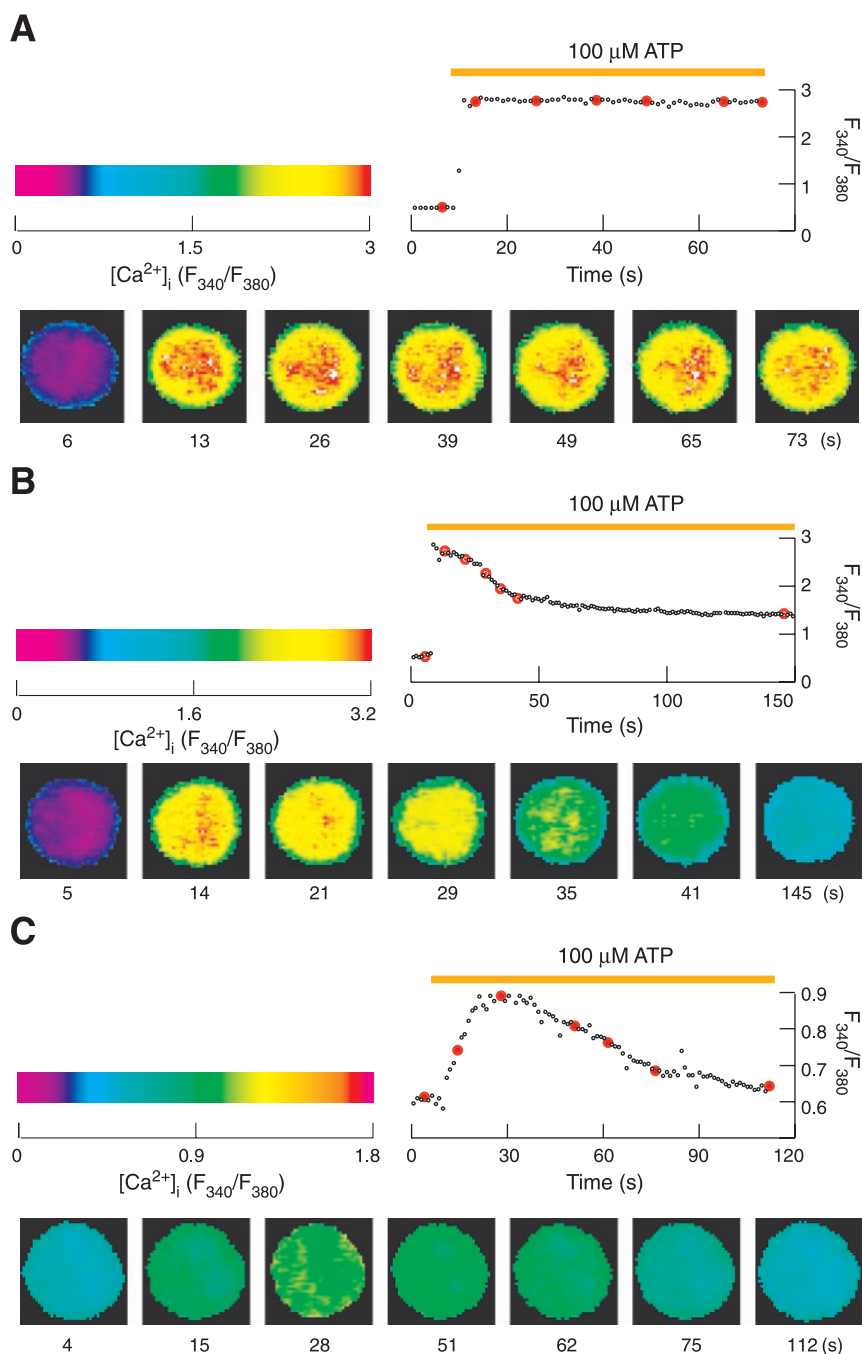


Fig. 7. Independence of spatial characteristics of Ca^{2+} signals in P2XR-expressing GT1 cells of the rate of receptor desensitization. Representative images for slow desensitizing P2X_{2a}R (A), moderate desensitizing P2X_{2b}R (B), and rapidly desensitizing P2X₃R (C). In each, *bottom* shows ratio (F_{340}/F_{380}) images of a single cell at 7 different time points. The pseudocolor scales are shown at *upper left*. *Upper right* shows temporal changes of $[\text{Ca}^{2+}]_i$ recorded from the whole cell area, and red circles correspond to images at *bottom*.

participate in the control of physiological processes by depolarizing the cells and activating voltage-gated Ca^{2+} influx (28), GT1 cells also provide a suitable cell model for studying the Ca^{2+} signaling function of these receptors. In general, the associated voltage-gated Ca^{2+} influx amplifies Ca^{2+} signals but does not influence the kinetics of signal desensitization. Here, this was illustrated in three types of experiments: depolarization of cells with high potassium, blockade of voltage-gated Ca^{2+} influx by nifedipine, and substitution of extracellular sodium with *N*-methyl-D-glucamine. Experiments with sodium-free media also illustrate that sodium conductance through the pore of P2XR is not critical for Ca^{2+} permeability of the pores.

When expressed as homomers in GT1 cells, both wild-type and chimeric channels responded to ATP with a global rise in $[\text{Ca}^{2+}]_i$ but with variable and receptor-specific peak amplitudes of Ca^{2+} response and rates of desensitization. The global nature of Ca^{2+} signals was observed during the rising and declining phases in $[\text{Ca}^{2+}]_i$, indicating that the rate of receptor desensitization did not affect the spatial characteristics of Ca^{2+} signals. For the majority of P2XRs, the rising phase was rapid and more difficult to study with Ca^{2+} imaging at the rate of about one image per second. The exception was P2X₇R, which responded to ATP with a rise in $[\text{Ca}^{2+}]_i$ that lasted for tens of seconds. On the other hand, the rate of Ca^{2+} imaging

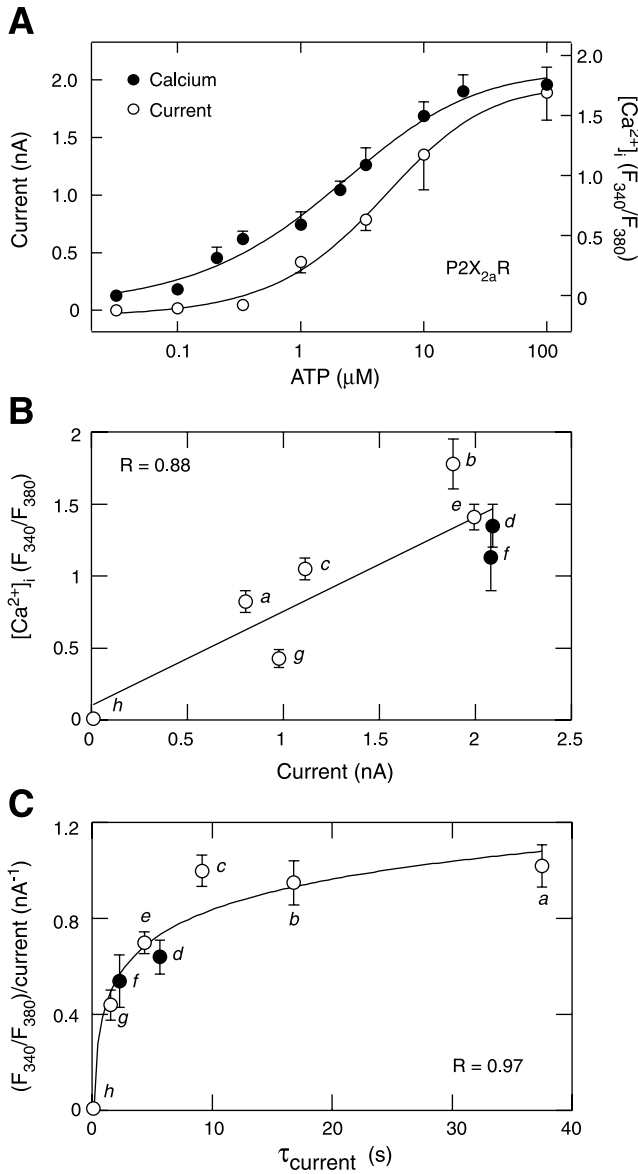


Fig. 8. The relationship between current and Ca^{2+} responses in P2XR-expressing cells. **A**: concentration-dependent effects of ATP on peak amplitude of current and Ca^{2+} responses in P2X_{2a}R-expressing cells. **B**: linear relationship between the peak amplitude of current and Ca^{2+} in P2XR-expressing cells in response to 100 μM ATP. **C**: log-linear relationship between τ values for decay in current response and peak amplitude of Ca^{2+} response to 100 μM ATP. To minimize the impact of the amplitude of current response on Ca^{2+} signaling, the values for peak $[Ca^{2+}]_i$ were normalized by dividing the F_{340}/F_{380} values with the peak values of the corresponding current response. *a*, P2X₇R; *b*, P2X_{2a}R; *c*, P2X₄R; *d*, P2X_{2a} + X₄R; *e*, P2X_{2b}R; *f*, P2X_{2b} + X₄R; *g*, P2X₃R; and *h*, vector-expressing cells. *R*, coefficient of correlation.

in our experiments was sufficient to follow the temporal aspects of Ca^{2+} signaling during the declining phase in all receptors, including the rapidly desensitizing P2X₃R.

The global Ca^{2+} signals are not only suitable to control the plasma membrane events but also the cytosolic and nuclear events (29). In that respect, the attenuation of the amplitude of global Ca^{2+} signals

could provide an effective mechanism for graded actions of P2XRs on cytosolic and nuclear processes. In general, the global Ca^{2+} signaling could be generated by Ca^{2+} influx by two mechanisms: passive diffusion of

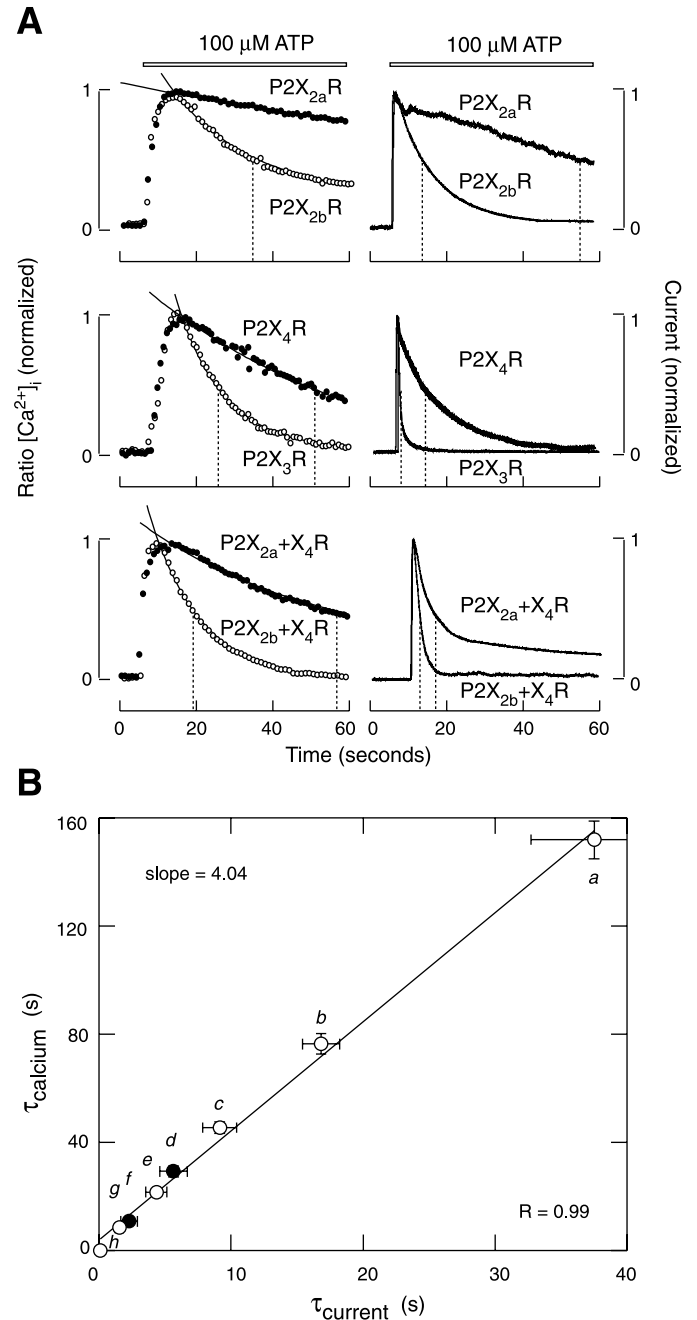


Fig. 9. Comparison of decays for Ca^{2+} and current signals in P2XR-expressing cells during the sustained stimulation with 100 μM ATP. **A**: the profiles of agonist-induced Ca^{2+} (left) and current (right) signals in cells expressing P2X_{2a}R and P2X_{2b}R (top), P2X₄R and P2X₃R (middle), and P2X_{2a} + X₄R and P2X_{2b} + X₄R (bottom). Vertical dotted lines indicate the values for τ . Means \pm SE for τ values are shown in Table 2. For easier comparison, the peak values for the $[Ca^{2+}]_i$ and current were normalized and currents were purposely shown in the opposite direction. **B**: correlation between τ values for decay in Ca^{2+} and current signals in P2XR-expressing cells in response to 100 μM ATP. Means \pm SE for τ values are shown in Table 2. *a*, P2X₇R; *b*, P2X_{2a}R; *c*, P2X₄R; *d*, P2X_{2a} + X₄R; *e*, P2X_{2b}R; *f*, P2X_{2b} + X₄R; *g*, P2X₃R; and *h*, vector-expressing cells.

Table 2. Receptor-specific half-times (τ) for desensitization of calcium and current responses during the prolonged stimulation with 100 μ M ATP

Receptor	τ (s) for calcium	τ (s) for current
P2X ₇ R	152.34 \pm 7.21(8)	37.53 \pm 4.81(5)
P2X _{2a} R	76.39 \pm 3.79(12)	16.82 \pm 1.39(14)
P2X ₄ R	45.43 \pm 2.04(11)	9.16 \pm 1.29(11)
P2X _{2a} + X ₄ R	29.19 \pm 1.93(7)	5.65 \pm 1.05(19)
P2X _{2b} R	21.54 \pm 0.99(14)	4.36 \pm 0.80(13)
P2X _{2b} + X ₄ R	10.74 \pm 0.65(5)	2.28 \pm 0.61(12)
P2X ₃ R	8.43 \pm 0.59(7)	1.55 \pm 0.32(19)

Numbers in parenthesis indicate number of single cells for current recordings or number of experiments with simultaneous calcium recordings from at least 15 cells per dish. Basal $[Ca^{2+}]_i$ and leak current values were subtracted.

ions within the cytosol and active propagation, known as Ca^{2+} -induced Ca^{2+} release, through ryanodine receptor channels (29). The second mechanism is unlikely, because ryanodine did not affect the pattern of P2XR-mediated Ca^{2+} signals and was also ineffective in altering the pattern of action potential-dependent Ca^{2+} signaling in these cells (5). This provides an additional methodological advantage for the usage of GT1 cells in studies on P2XR activity.

In this study, we also progressed in understanding the mechanism for generating the receptor-specific Ca^{2+} signaling patterns. Linear regression analysis revealed the correlation between peak amplitudes of current and Ca^{2+} response, suggesting that the size of inwardly depolarizing current reflected on the amplitude of Ca^{2+} response. Experiments with P2X_{2a}R stimulated with increasing concentrations of ATP are also in line with this hypothesis. From a physiological point

of view, variations in single-channel conductivity of P2XRs (10, 11, 46) and the receptor-specific conductivity for Ca^{2+} (12, 13, 35, 39, 42) should be the major sources contributing to the variations in the peak amplitude of current response among receptors, if they are expressed at comparable levels. To account for impact of the size of current on Ca^{2+} signaling, the peak amplitudes of Ca^{2+} responses were normalized and plotted against τ values for decay in current response. The results of these investigations indicate a linear-log relationship between the two parameters. Therefore, the rate of current desensitization is also likely to influence the magnitude of Ca^{2+} response.

Furthermore, we show that the patterns of current and Ca^{2+} signal decays are highly comparable. Linear regression analysis revealed a strong correlation between the τ values for current and Ca^{2+} signals, indicating that rates of current desensitization also determine the rates of Ca^{2+} signal desensitization. This in turn suggests that both measurements could be used to compare the rates of receptor desensitization. For example, the same conclusion would be reached in analysis of the dependence of receptor desensitization on ectodomain structure by comparing wild-type P2X_{2a}R and P2X_{2b}R and chimeric P2X_{2a} + X₄R and P2X_{2b} + X₄R pairs in current and Ca^{2+} measurements.

However, the times needed to reach the half- and steady desensitized states for P2XRs were significantly longer in Ca^{2+} than in current measurements. Slower Ca^{2+} signal desensitization reflects the slow kinetics of cation elimination from the cytosol. The present data confirmed that Ca^{2+} handling is not a channel- but rather a cell-dependent process. In general, Ca^{2+} is removed from the cytosol by several mechanisms, in-

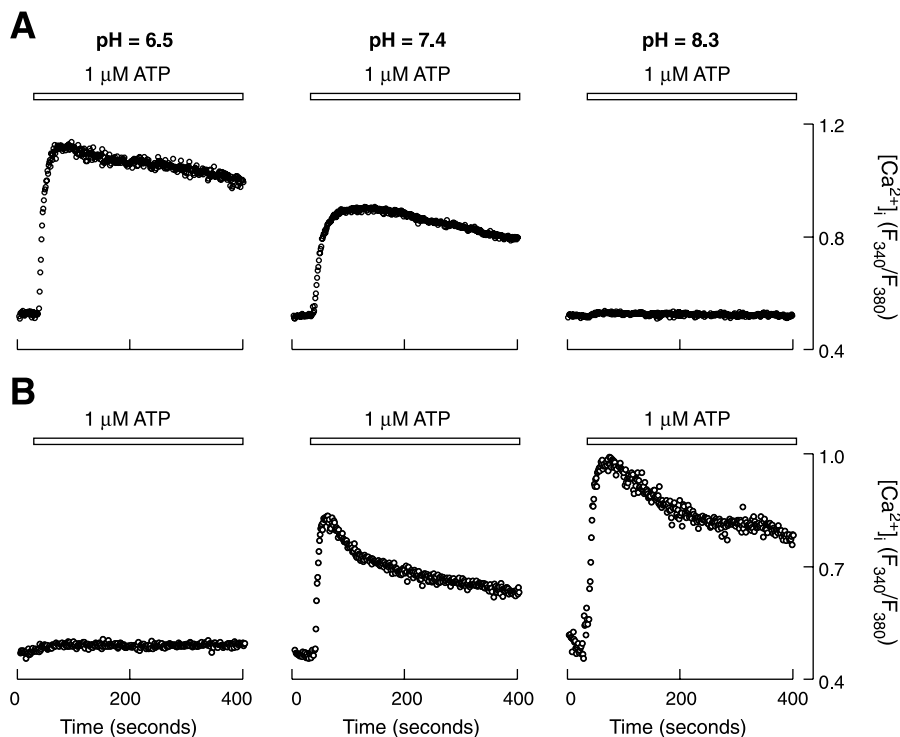


Fig. 10. Receptor-specific sensitivity of 1 μ M ATP-induced Ca^{2+} signals in GT1 cells to pH. A: P2X_{2a}R; B: P2X₄R. The traces shown are mean values from at least 15 records in representative experiments.

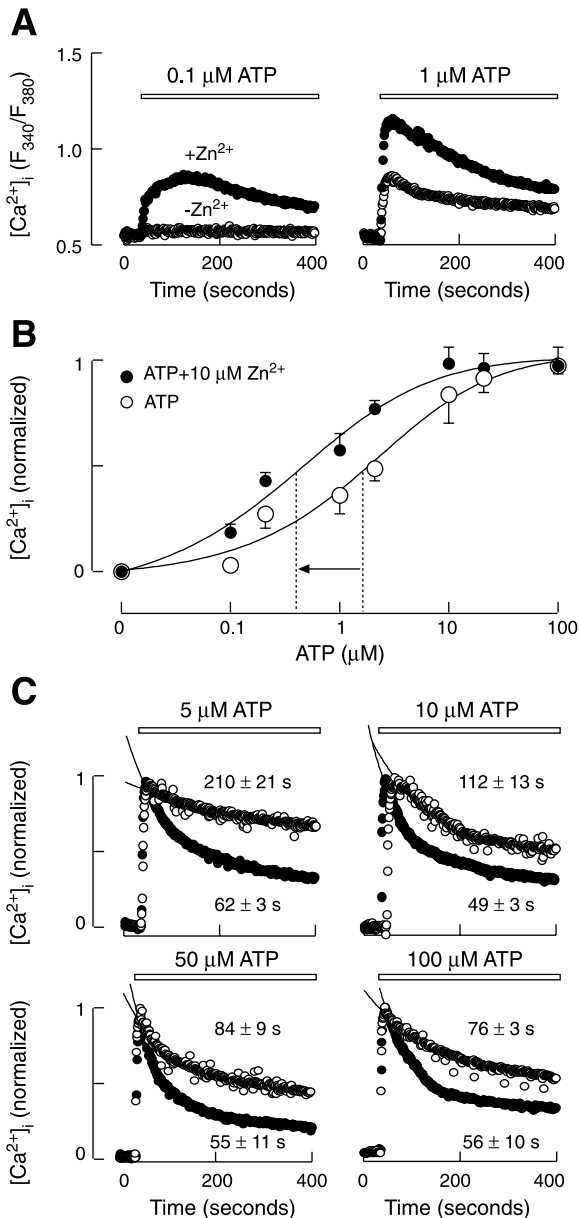


Fig. 11. Zn²⁺ modulates ATP-induced activity of P2X_{2a}R. **A**: representative traces of ATP-induced Ca²⁺ signals in the presence and absence of 10 μM Zn²⁺. **B**: leftward shift in concentration dependence of ATP on peak amplitude of Ca²⁺ signals. **C**: the extracellular Zn²⁺-dependent increases in the rates of signal desensitization. Traces shown are means for at least 20 cells in representative experiments, and numbers are means \pm SE for τ values from at least 3 experiments.

cluding Na⁺/Ca²⁺ exchanger, plasma membrane and endoplasmic reticulum membrane Ca²⁺-ATPases, and uptake of Ca²⁺ by mitochondria (29). In this respect, it is reasonable to speculate that the ratio between τ values for current and Ca²⁺ could vary among variable cells, depending on the cell type-specific Ca²⁺ handling mechanisms.

Finally, our results show that Ca²⁺ signals reflect well the receptor-specific pharmacology. We have previously reported that agonists other than ATP stimulate Ca²⁺ influx in GT1 cells in a receptor-specific

manner and with EC₅₀ values comparable to those in current measurements (16, 17, 23). Here, we show that EC₅₀ values for ATP estimated in current and Ca²⁺ responses are comparable. Our results further indicate that Ca²⁺ measurements report accurately about the receptor-specific sensitivity to extracellular pH and Zn²⁺, found previously by others in current (1, 7–9, 34, 44, 45) and Ca²⁺ (47) measurements. Experiments with Zn²⁺ are also in accord with our recent findings that the ectodomain structures of P2XRs, i.e., the efficacy of agonist for receptors, influence the rates of receptor desensitization (16, 17). Thus a leftward shift in the EC₅₀ for ATP in P2X_{2a}R-expressing cells bathed in Zn²⁺-containing medium increased the rates of receptor desensitization.

In conclusion, here we show that recombinant P2XRs can generate global Ca²⁺ signals when expressed as homomers in GT1 cells. Ca²⁺ influx through the pores of P2XRs and voltage-gated Ca²⁺ channels, and the subsequent diffusion of this cation within the cell, accounts for the generation of global signals. This is a common feature of all P2XRs, whereas the peak amplitude of Ca²⁺ response and the temporal aspects of Ca²⁺ signaling are receptor specific. Parallelism in current and Ca²⁺ signaling patterns observed under different experimental conditions also indicate the potential application of single-cell Ca²⁺ measurements in studies of activity of P2XRs. There are several advantages of single-cell Ca²⁺ measurements in such studies, including the number of cells that can be examined simultaneously, the preserved interior of the cells compared with the whole cell patch-clamp recording, and the possibility of studying the spatial aspects of signaling and physiological role of P2XRs in intact cells. This method also has its limitations, including the temporal dissociation between Ca²⁺ signaling and P2XR activity and the selection of a cell model with respect to the endogenous expression of P1 and P2YRs, the coupling of Ca²⁺ influx to Ca²⁺-induced Ca²⁺ release from intracellular stores, and the cell type specificity in pathways controlling Ca²⁺ efflux.

Present addresses: H. Zemkova, Institute of Physiology, Academy of Sciences of the Czech Republic, 142 20 Prague4, Czech Republic; T.-a. Koshimizu, Dept. of Molecular Cellular Pharmacology, NCMRC, Tokyo 154, Japan.

REFERENCES

1. Acuna-Castillo C, Morales B, and Huidobro-Toro JP. Zinc and copper modulate differentially the P2X₄ receptor. *J Neurochem* 74: 1529–1537, 2000.
2. Bianchi BR, Lynch KJ, Touma E, Niforatos W, Burgard EC, Alexander KM, Park HS, Yu H, Metzger R, Kowaluk E, Jarvis MF, and van Biesen T. Pharmacological characterization of recombinant human and rat P2X receptor subtypes. *Eur J Pharmacol* 376: 127–138, 1999.
3. Brake AJ, Wagenbach MJ, and Julius D. New structural motif for ligand-gated ion channels defined by an ionotropic ATP receptor. *Nature* 371: 519–523, 1994.
4. Buell G, Lewis C, Collo G, North RA, and Surprenant A. An antagonist-insensitive P2X receptor expressed in epithelia and brain. *EMBO J* 15: 55–62, 1996.

5. **Charles AC and Hales TG.** Mechanisms of spontaneous calcium oscillations and action potentials in immortalized hypothalamic (GT1-7) neurons. *J Neurophysiol* 73: 56–64, 1994.
6. **Chen CC, Akoplan AN, Sivlott L, Colquhoun D, Burnstock G, and Wood JN.** A P2X purinoreceptor expressed by a subset of sensory neurons. *Nature* 377: 428–431, 1995.
7. **Clarke CE, Benham CD, Bridges A, George AR, and Meadows HJ.** Mutation of histidine 286 of the human P2X₄ purinoreceptor removes extracellular pH sensitivity. *J Physiol* 523: 697–703, 2000.
8. **Clyne JD, Brown TC, and Hume RI.** Expression level dependent changes in the properties of P2X₂ receptors. *Neuropharmacology* 44: 403–412, 2003.
9. **Clyne JD, LaPointe LD, and Hume RI.** The role of histidine residues in modulation of the rat P2X₂ purinoreceptor by zinc and pH. *J Physiol* 539: 347–359, 2002.
10. **Ding S and Sachs F.** Single channel properties of P2X₂ purinoreceptors. *J Gen Physiol* 113: 695–719, 1999.
11. **Evans RJ.** Single channel properties of ATP-gated cation channels (P2X receptors) heterologously expressed in Chinese hamster ovary cells. *Neurosci Lett* 212: 212–214, 1996.
12. **Evans RJ, Lewis C, Virginio C, Lundstrom K, Buell G, Surprenant A, and North RA.** Ionic permeability of, and divalent cation effects on, two ATP-gated cation channels (P2X receptors) expressed in mammalian cells. *J Physiol* 497: 413–422, 1996.
13. **Garcia-Guzman M, Soto F, Gomez-Hernandez JM, Lund PE, and Stuhmer W.** Characterization of recombinant human P2X₄ receptor reveals pharmacological differences to the rat homologue. *Mol Pharmacol* 51: 109–118, 1997.
14. **Haines WR, Migita K, Cox JA, Egan TM, and Voigt MM.** The first transmembrane domain of the P2X receptor subunit participates in the agonist-induced gating of the channel. *J Biol Chem* 276: 32793–32798, 2001.
15. **Hamill OP, Marty A, Neher E, Sakmann B, and Sigworth FJ.** Improved patch-clamp techniques for high-resolution current recording from cells and cell-free membrane patches. *Pflügers Arch* 391: 85–100, 1981.
16. **He ML, Koshimizu T, Tomić M, and Stojilkovic SS.** Purinergic P2X₂ receptor desensitization depends on coupling between ectodomain and C-terminal domain. *Mol Pharmacol* 62: 1187–1197, 2002.
17. **He ML, Zemkova H, and Stojilkovic SS.** Dependence of purinergic P2X receptor activity on ectodomain structure. *J Biol Chem* 278: 10182–10188, 2003.
18. **King BF, Wildman SS, Zinanshina LE, Pintor J, and Burnstock G.** Effects of extracellular pH on agonism and antagonism at recombinant P2X₂ receptor. *Br J Physiol* 121: 1445–1453, 1997.
19. **Koshimizu T, Koshimizu M, and Stojilkovic SS.** Contributions of the C-terminal domain to the control of P2X receptor desensitization. *J Biol Chem* 274: 37651–37657, 1999.
20. **Koshimizu T, Tomić M, Koshimizu M, and Stojilkovic SS.** Identification of amino acid residues contributing to desensitization of the P2X₂ receptor channel. *J Biol Chem* 273: 12853–12857, 1998.
21. **Koshimizu T, Tomić M, Van Goor F, and Stojilkovic SS.** Functional role of alternative splicing in pituitary P2X₂ receptor-channel activation and desensitization. *Mol Endocrinol* 12: 901–913, 1998.
22. **Koshimizu T, Tomić M, Wong AOL, Zivadinovic D, and Stojilkovic SS.** Characterization of purinergic receptors and receptor-channels expressed in anterior pituitary cells. *Endocrinology* 141: 4091–4099, 2000.
23. **Koshimizu T, Ueno S, Tanoue A, Yanagihara N, Stojilkovic SS, and Tsujimoto G.** Heteromultimerization modulates P2X receptor functions through participating extracellular and C-terminal subdomains. *J Biol Chem* 277: 46891–46899, 2002.
24. **Koshimizu T, Van Goor F, Tomić M, Wong AOL, Tanoue A, Tsujimoto G, and Stojilkovic SS.** Characterization of calcium signaling by purinergic receptor-channels expressed in excitable cells. *Mol Pharmacol* 58: 936–945, 2000.
25. **Krsmanovic LZ, Mores N, Navarro C, Arora KK, and Catt KJ.** An agonist-induced switch in G protein coupling of the gonadotropin-releasing hormone receptor regulates pulsatile neuropeptide secretion. *Proc Natl Acad Sci USA* 100: 2969–2974, 2003.
26. **Le KT, Boue-Grabot E, Archambault V, and Seguela P.** Functional and biochemical evidence for heteromeric ATP-gated channels composed of P2X₁ and P2X₅ subunits. *J Biol Chem* 274: 15415–15419, 1999.
27. **Lewis C, Neidhart S, Holy C, North RA, Buell G, and Surprenant A.** Coexpression of P2X₂ and P2X₃ receptor subunits can account for ATP-gated currents in sensory neurons. *Nature* 377: 432–435, 1995.
28. **North RA.** Molecular physiology of P2X receptors. *Physiol Rev* 82: 1013–1067, 2002.
29. **Nowycky MC and Thomas AP.** Intracellular calcium signaling. *J Cell Sci* 115: 3715–3716, 2002.
30. **Ralevic V and Burnstock G.** Receptors for purines and pyrimidines. *Pharmacol Rev* 50: 413–492, 1998.
31. **Schachter JB, Sromek SM, Nicholas RA, and Harden TK.** HEK293 human embryonic kidney cells endogenously express the P2Y₁ and P2Y₂ receptors. *Neuropharmacology* 36: 1181–1187, 1997.
32. **Schilling WP, Sinkins WG, and Estacion M.** Maitotoxin activates a nonselective cation channel and a P2Z/P2X7-like cytolytic pore in human skin fibroblast. *Am J Physiol Cell Physiol* 277: C755–C765, 1999.
33. **Soto F, Garcia-Guzman M, Gomez-Hernandez JM, Hollmann M, Karschin C, and Stuhmer W.** P2X₄: An ATP-activated ionotropic receptor cloned from rat brain. *Proc Natl Acad Sci USA* 93: 3684–3688, 1996.
34. **Stoop R, Surprenant A, and North RA.** Different sensitivities to pH of ATP-induced currents at four cloned P2X receptors. *J Neurophysiol* 78: 1837–1840, 1997.
35. **Surprenant A, Rassendren F, Kawashima E, North RA, and Buell G.** The cytosolic P_{2Z} receptor for extracellular ATP identified as a P_{2X} receptor (P2X₇). *Science* 272: 735–738, 1996.
36. **Surprenant A, Schneidr DA, Wilson HL, Galligan JJ, and North RA.** Functional properties of heteromeric P2X_{1/5} receptors expressed in HEK cells and excitatory junction potential in guinea-pig submucosal arterioles. *J Auton Nerv Sistem* 81: 249–263, 2000.
37. **Tomić M, Jobin RM, Vergara LA, and Stojilkovic SS.** Expression of purinergic receptor channels in their role in calcium signaling and hormone release in pituitary gonadotrophs. *J Biol Chem* 271: 21200–21208, 1996.
38. **Troadee JD, Thirion S, Nicaise G, Lemos JR, and Dayanithi G.** ATP-evoked increases in [Ca²⁺]_i and peptide release from rat isolated neurohypophysial terminals via P2X₂ purinoreceptor. *J Physiol* 511: 89–103, 1998.
39. **Valera S, Hussy N, Evans RJ, Adami N, North A, Surprenant A, and Buell G.** A new class of ligand-gated ion channel defined by P_{2X} receptor for extracellular ATP. *Nature* 371: 516–519, 1994.
40. **Van Goor F, Krsmanovic LZ, Catt KJ, and Stojilkovic SS.** Control of action potential-driven calcium influx in GT1 neurons by the activation status of sodium and calcium channels. *Mol Endocrinol* 13: 587–603, 1999.
41. **Van Goor F, Krsmanovic LZ, Catt KJ, and Stojilkovic SS.** Coordinate regulation of gonadotropin-releasing hormone neuronal firing patterns by cytosolic calcium and store depletion. *Proc Natl Acad Sci USA* 96: 4101–4106, 1999.
42. **Virginio G, North RA, and Surprenant A.** Calcium permeability and block at homomeric and heteromeric P2X₂ and P2X₃ receptors, and P2X receptors in rat nodose neurones. *J Physiol* 510: 22–35, 1998.
43. **White SM, Imig JD, Kim TT, Hauschild BC, and Inscho EW.** Calcium signaling pathways utilized by P2X receptors in freshly isolated preglomerular MVSMC. *Am J Physiol Renal Physiol* 280: F1054–F1061, 2001.

44. **Wildman SS, King BF, and Burnstock G.** Modulation of ATP-responses at recombinant rP2X₄ receptors by extracellular pH and zinc. *Br J Pharmacol* 126: 762–768, 1999.
45. **Xiong K, Peoples RW, Mntgomery JP, Chiang Y, Steward RR, Weight FF, and Li C.** Differential modulation by copper and zinc of P2X₂ and P2X₄ receptor function. *J Neurophysiol* 81: 2088–2094, 1999.
46. **Zhou Z and Hume RI.** Two mechanisms for inward rectification of current flow through the purinoreceptor P2X₂ class of ATP-gated channels. *J Physiol* 507: 353–364, 1998.
47. **Zsembery A, Boyce AT, Liang L, Peti-Peterdi J, Bell PD, and Schwiebert EM.** Sustained Ca²⁺ entry through P2X nucleotide receptor channels in human airway epithelial cells. *J Biol Chem* 278: 13398–13408, 2003.

